

Performance and properties of e-beam pumped XeF(C+A) lasers

W. L. Nighan

United Technologies Research Center, East Hartford, CT 06108

G. Marowsky

Max-Planck Institute für Biophysikalische Chemie, Goettingen, FRG

R. A. Sauerbrey, F. K. Tittel, W. L. Wilson Jr., and Y. Zhu

Department of Electrical Engineering, Rice University, Houston, TX 77251

Abstract

Efficient, ultra-narrow spectral output from an electron-beam excited XeF(C+A) laser medium has been achieved by injection controlled tuning. Using a two-component buffer gas comprised of Ar and Kr, XeF(C+A) laser pulse energy and intrinsic efficiency values comparable to those of UV rare gas-halide lasers have been demonstrated. For a 482.5 nm injection wavelength that is well matched to the XeF(C+A) gain maximum, output energy density and intrinsic efficiency values of approximately 8 J/liter and 6% were achieved.

Introduction

The XeF(C+A) excimer transition is unique among those of the rare gas-halide (RGH) class because of its blue-green wavelength and exceptionally broadband fluorescence spectrum. Recent advances indicate that the electrically excited XeF(C+A) medium has considerable potential for development as an efficient, optical source that is tunable throughout the entire blue-green region of the spectrum¹. In this paper we report on our efforts to capitalize on these characteristics by injection control of an XeF(C+A) amplifier. The injection source used was a dye laser tunable throughout the entire blue-green spectral region and having a spectral width of only 0.001 nm. In addition, we have demonstrated the merits of using two rare gas components to form the buffer gas. Notable success has been realized using an Ar-Kr combination to form the high pressure buffer for the XeF(C+A) laser medium². This approach has resulted in a dramatic improvement in the net gain of the broadband XeF(C+A) transition centered at ~ 480 nm. Indeed, laser pulse energy density and intrinsic efficiency values have been demonstrated that compare very favorably with those of the more highly developed UV RGH B+X lasers, by using the XeF(C+A) medium either as a broadband oscillator, or as a wavelength selectable amplifier.

Experimental details

The experimental apparatus used in this work is illustrated in Figure 1. A Physics International Pulserad 110 electron beam generator was used to transversely excite high pressure gas mixtures^{1,2}. The electron beam energy was 1 MeV, and the excitation pulse duration was 10 nsec (FWHM), producing a pump energy density of ~ 135 J/liter, as measured by a calorimeter and Faraday cup probe. The stainless steel reaction cell was carefully passivated by prolonged exposure to F₂. High purity gas mixtures comprised of NF₃, F₂, Xe, Kr and Ar were used. Good gas mixing of the components was found to be essential, and was obtained using turbulent flow of the high pressure gas components into the reaction cell. Each fresh gas mixture could be used for about 10 shots before performance degradation became significant.

Injection control system

An excimer-pumped dye laser system (Lambda Physik Model EMG 101E/FL2002) having a bandwidth of ~ 5×10^{-3} nm was used to provide injection control¹. Use of an intracavity etalon resulted in significant additional bandwidth reduction to 9×10^{-4} nm. This seed oscillator delivered an output of up to 8 mJ in a 10 nsec pulse (FWHM), tunable from 430 nm to 550 nm using Coumarin dyes 2, 102 and 307. A telescope was used to reduce the injection beam diameter so that most of the available dye laser pulse energy entered the unstable cavity of the e-beam pumped cell (Figure 1).

The temporal evolution of the free running laser, the dye laser and the injection controlled XeF(C+A) laser output, illustrated in Figure 2, were monitored by a fast vacuum photodiode detector [ITT-F4000 (S5)]. Neutral density filters were used to avoid saturation of the photodiode and color glasses were used to define the spectral region of interest. Signals were recorded by a Tektronix R7912 transient digitizer. The time resolution of the entire system was better than 2 nsec. The temporally integrated, spectrally resolved laser signal was recorded by an optical multi-channel analyzer (OMA III), using a Jarrell-Ash 0.25 meter spectrometer having a spectral resolution of about 0.3 nm. Additionally, the temporal relationship of the dye laser and \underline{e} -beam pulse was monitored by a storage oscilloscope. The timing relationship between the dye laser and \underline{e} -beam was adjusted by timing circuits so that the volume filling pass of the injected dye laser pulse overlapped the rise of the XeF(C+A) temporal gain profile.

Cavity optics

The optical cavity used in these studies was a positive-branch confocal unstable, intracell resonator, consisting of a concave end mirror with an injection hole of 1.5 mm diameter and a coating having a high reflectivity in the blue-green region, and a convex output coupler (Figure 1). The mirrors, having focal lengths of f_2 and $-f_1$, respectively, were separated by a distance $L = f_2 - f_1$, typically about 12 cm for our conditions, with the magnification given by the relation, $M = f_2/f_1$. Various cavities were examined having magnifications ranging from 1.05 to 1.23¹. The output coupler was a meniscus lens of zero refraction power having a highly reflective coated spot on the convex side with a diameter, d , of 1.4 cm. The active region was a cylindrical volume defined by the \underline{e} -beam pumping length (10 cm) and the clear aperture having a diameter $d \times M$ cm. For these conditions the role of the cavity was to serve as a beam expanding telescope of a regenerative amplifier^{1,3}.

XeF(C+A) gain profile

The addition of Kr to XeF(C+A) laser mixtures has been found to result in a significantly improved gain profile when \underline{e} -beam excitation is used^{2,4}. Presented in Figure 3 is the measured temporal evolution of the net gain for representative XeF(C+A) laser mixtures with and without Kr. The fractional concentrations of each constituent of the Ar-Xe-NF₃-F₂ mixture are optimized and result in broadband extraction energy density values typically in the 1.0 -1.5 J/liter range when a free running stable resonator is used. However, Figure 3 vividly illustrates the significant reduction in the initial absorption and the increase in peak gain when Kr is added to the mixture and all constituent fractional concentrations are re-optimized. The improved gain profile typical of Kr-containing mixtures has been found to increase the broadband output energy and intrinsic efficiency of a stable, free running oscillator to levels comparable to those of the UV XeF(B+X) transition⁴. The wavelength dependence of the peak values of gain and initial absorption for mixtures with and without Kr are presented in Figure 4.

Wavelength tuning

In order to determine the range within which the XeF(C+A) medium can be efficiently tuned, the wavelength of the injected dye laser pulse was varied from 435 nm to 535 nm. Figure 5 provides an illustrative comparison of the spectra of several, separate injection controlled shots and a free running oscillator spectrum, along with the XeF(C+A) fluorescence spectrum. Because of the large cavity loss associated with the unstable resonator optics used, the maximum free running output energy was always less than 0.1 mJ for these conditions. However, several mJ of amplified output was obtained for injection wavelengths as low as 459.4 nm and as high as 505 nm. In fact, amplification of the injected signal was observed for wavelengths as low as 435 nm and as high as 535 nm.

Presented in Figure 6 is the measured output energy as a function of wavelength for several different cavities, along with a typical free running spectrum for comparison. The specific injection wavelengths were chosen to correspond to the peaks and absorption valleys that are always apparent in the free running XeF(C+A) laser spectrum. This figure shows that the wavelength dependence of the minima observed in the amplified output correlates reasonably well with the locations of the absorption valleys in the free running spectrum. The discrete absorption is due primarily to phototransitions from Xe(³P₂, ³P₁) atoms to higher Rydberg levels.

Output energy and efficiency

For the conditions of Figures 5 and 6 the e-beam energy deposition was measured and found to be approximately 135 J/liter, a value consistent with calculated and measured values of medium properties⁵. Since the active volume defined by the mirror spacing and magnification values varied from 16.8 cm³ to 20.4 cm³ for our conditions, the maximum 149 mJ output obtained at 482.5 nm (Figure 6) corresponds to an energy density of ~ 8 J/liter and an intrinsic efficiency of approximately 6%. On a volumetric basis these values are actually higher than those typical of room temperature XeF(B+X) laser operation, and are comparable to XeF(B+X) performance at the 450°K temperature found to be optimum for that laser^{6,7}. This is rather surprising in view of the fact that the C+A quantum efficiency is ~ 25% less than that of the B+X transition. However, because of the strongly repulsive nature of the XeF(A) state, the C+A laser does not suffer from lower level population buildup as is the case with the B+X laser. Additionally, the 6.5 atm Ar-Kr buffer mixture used in the present work results in B-C state mixing and vibrational relaxation times of approximately 0.1 nsec, which are very much less than those typical of optimum B+X laser mixtures using Ne as the buffer at pressures of ~ 3 atm. Since both lower level buildup and slow vibrational relaxation can adversely affect XeF(B+X) laser energy and efficiency, apparently the XeF(C+A) medium has advantages in this regard, provided the level of broadband transient absorption is controlled kinetically and the characteristically slow build-up of optical flux that usually limits oscillator performance is overcome by using the C+A medium as an amplifier.

Bleaching of absorbers

In addition to the effects described above, bleaching of transient absorbing species exerts an exceptionally strong influence on XeF(C+A) laser performance, an effect that appears to be relatively of little importance in B+X rare gas-halide lasers. Presented in Figure 7 are the cross sections for stimulated emission of the XeF(C+A) transition and those of several rare gas-halide B+X transitions, along with the absorption cross sections of several transient species typical of rare gas-halides laser mixtures. Because the cross sections for the dominant blue-green absorbing species⁵ are larger than the cross section for stimulated emission of the XeF(C+A) transition, and since the saturation fluxes are comparable, bleaching of the transient absorption is a very significant effect for the high intracavity flux levels typical of the present experiment. Further, there appear to be no non-saturable absorbers in the XeF(C+A) laser mixture. In contrast, the B+X stimulated emission cross sections are much larger than the UV absorption cross sections of transient species. Thus, while it is much easier to achieve higher gain on the B+X transitions, the presence of non-saturable transient absorption imposes a limit on B+X laser extraction efficiency.

Effects of Kr

Detailed spectral analysis of various gas mixtures with and without Kr led to the conclusion that the primary effect of Kr addition to XeF(C+A) laser mixtures was a significantly lower level of transient absorption in the blue-green spectral region⁴. However, there is also evidence of additional factors that benefit XeF(C+A) laser performance², including: (1) faster mixing of the XeF B and C states; (2) a contribution to the net gain in the 400-450 nm region due to the presence of a high concentration of the Kr₂F excimer; and (3) a large increase in absorption at UV wavelengths, also due to Kr₂F, which suppresses oscillation on the competitive XeF(B+X) transition and, for certain conditions, makes possible relatively efficient, simultaneous oscillation of the XeF(B+X) and XeF(C+A) laser transitions.

Presented in Figure 8 is the time integrated fluorescence in the 300-600 nm region for representative XeF(C+A) laser mixture conditions. This figure shows clearly the contribution due to the presence of the Kr₂F excimer. The fact that the XeF(C) and Kr₂F populations are comparable² in XeF(C+A) mixtures containing Kr suggests that Kr₂F may be making a contribution to the gain on the short wavelength side of the laser spectrum. However, the broader spectral width, longer natural lifetime, and shorter wavelength of Kr₂F compared to XeF(C+A) results in a stimulated emission cross section that we estimate to be only ~ 2.5 x 10⁻¹⁸ cm² at its peak at 400 nm, a value approximately one fourth that of the XeF(C+A) transition. Thus, any influence of Kr₂F on the gain for wavelengths > 480 nm must be quite small.

Other factors also have to be considered, however. Figure 9 presents the temporal evolution of both the Kr_2F and $\text{XeF}(\text{C}+\text{A})$ fluorescence spectra, showing that the peak in the Kr_2F fluorescence precedes that of $\text{XeF}(\text{C}+\text{A})$ by 15-20 nsec. Therefore, even though its stimulated emission cross section is small, a large Kr_2F population favors an earlier buildup of gain for wavelengths to the short wavelength side of the $\text{XeF}(\text{C}+\text{A})$ gain maximum. For example, based on the data of Figures 8 and 9 we estimate that the Kr_2F contribution to the peak gain at ~ 450 nm could be as high as 10-20%. Such an effect could be significant when the $\text{C}+\text{A}$ gain medium is used as a wavelength tuned amplifier. This line of reasoning suggests that any increase in the gain of the $\text{XeF}(\text{C}+\text{A})$ laser medium due to the presence of Kr_2F should be observable only on the short wavelength side of the laser spectrum. In fact, comparison of free running laser spectra for Ar and Ar-Kr buffered mixtures shows a $\sim 50\%$ greater increase in the $\text{XeF}(\text{C}+\text{A})$ laser intensity around 470 nm than at 490 nm when Kr is added.

Simultaneous UV/visible laser oscillation

Although more than 95% of the total $\text{XeF}(\text{B},\text{C})$ population resides in the C state for the conditions of present interest, since the stimulated emission cross section for $\text{XeF}(\text{B}+\text{X})$ is $3 - 4 \times 10^{-16} \text{cm}^2$, the intense pumping required to produce adequate $\text{XeF}(\text{C}+\text{A})$ net gain usually results in even larger transient gain at the $\text{XeF}(\text{B}+\text{X})$ 351 nm wavelength. Thus, even though steps can be taken in the design of the $\text{C}+\text{A}$ cavity to minimize the possibility of $\text{B}+\text{X}$ oscillation, the $\text{B}+\text{X}$ gain is frequently so high that amplified stimulated emission of the $\text{B}+\text{X}$ transition occurs thereby depleting the gain on the desired $\text{C}+\text{A}$ transition. We capitalized on this characteristic in order to demonstrate the feasibility of simultaneous UV/visible laser oscillation on both the $\text{B}+\text{X}$ and $\text{C}+\text{A}$ transitions of the XeF excimer². A cavity optimized for laser oscillation at 351 nm and at 480 nm was used. The cavity was comprised of a mirror having nearly total reflectivity in the UV and blue-green regions, and a multiple coating outcoupler having a transmission of 20% at ~ 350 nm and 10% between 460 and 510 nm. Figure 10 presents the measured laser pulse energy densities for the UV and blue-green transitions of XeF as a function of Kr pressure, obtained using this dual wavelength cavity for conditions otherwise similar to those described previously. With no Kr in the mixture and using a $\text{C}+\text{A}$ cavity alone, previously these conditions resulted in $\text{C}+\text{A}$ laser pulses having an energy density of approximately 1 J/liter⁴. However, Figure 10 shows that when the optimized dual-wavelength cavity is used, no $\text{C}+\text{A}$ laser oscillation is observed in the absence of Kr, but the $\text{B}+\text{X}$ transition oscillates with an output pulse energy density of ~ 1 J/liter, a relatively high energy density level considering that the mixture used is very different from that found to be optimum for the $\text{XeF}(\text{B}+\text{X})$ laser,^{6,7}. Addition of Kr results in an immediate decrease in $\text{B}+\text{X}$ output, followed by simultaneous oscillation of the UV and visible transitions, and eventually $\text{C}+\text{A}$ oscillation alone for Kr pressures above ~ 300 Torr.

UV absorption

The decrease in $\text{B}+\text{X}$ laser energy (Figure 10) upon addition of Kr is the result of a reduction in the $\text{XeF}(\text{B})$ population relative to that of $\text{XeF}(\text{C})$ ², and, perhaps more significantly, because of the likelihood of a strong increase in absorption at ~ 351 nm due to the presence of Kr_2F . The Kr_2F population estimates based on the data of Figures 8 and 9 indicate that a Kr partial pressure as low as 50 Torr is likely to result in a very significant Kr_2F contribution to absorption at 351 nm. We feel that this is the primary cause of the decrease in $\text{XeF}(\text{B}+\text{X})$ laser output as Kr is added (Figure 10). This trend continues as Kr pressure is increased and for Kr pressures above about 150 Torr, for which the presence of Kr results in a reduction in absorption in the blue-green region^{2,4}, significant laser output is obtained from the $\text{C}+\text{A}$ transition. For Kr pressure between about 150-250 Torr combined UV/visible output in excess of 0.5 J/liter is obtained using the cavity optimized at both the $\text{B}+\text{X}$ and $\text{C}+\text{A}$ wavelengths, corresponding to an intrinsic efficiency of $\sim 0.4\%$. However, as the Kr pressure is increased above ~ 300 Torr, for which optimum $\text{C}+\text{A}$ performance has been demonstrated^{2,4}, the $\text{B}+\text{X}$ output decreases to a very low level. For this condition the beneficial influence of Kr on $\text{C}+\text{A}$ laser performance is at its maximum, while the peak absorption at 351 nm due to Kr_2F is estimated² on the basis of the Kr_2^+ absorption cross section to be on the order of $10\% \text{cm}^{-1}$. In view of the fact that the cavity used for this demonstration was specifically designed to support $\text{XeF}(\text{B}+\text{X})$ oscillation (Figure 10), we interpret these results as strong evidence that the two component Ar-Kr buffer used to optimize $\text{XeF}(\text{C}+\text{A})$ laser performance alone, when used with $\text{C}+\text{A}$ optics, significantly reduces the possibility of competitive oscillation on the parasitic $\text{B}+\text{X}$ transition, a particularly important consideration for the design of efficient $\text{XeF}(\text{C}+\text{A})$ lasers.

Summary

The results of this investigation show that the electrically excited XeF(C+A) medium using a synthesized Ar-Kr buffer has significant potential for development as an efficient optical source of high brightness that is tunable throughout a large portion of the blue-green spectral region. Moreover, the unusually high values of extraction energy density and of intrinsic efficiency that were obtained for an injection wavelength matched to the maximum gain, suggest that the XeF(C+A) medium may have the potential to rival its UV rare gas-halide counterparts for certain selected applications requiring high energy and efficiency.

Although relatively efficient ($> 0.1\%$) tuning has been demonstrated for wavelengths as low as 459.4 nm and as high as 505 nm, XeF(C+A) amplifier performance has been limited in the present investigation by the combination of a short active length (~ 10 cm) and undesirably low values of cavity magnification (< 1.3) required to compensate for the former. However, it is clear that these factors do not represent fundamental limitations. Considering that the gain of the e-beam excited XeF(C+A) medium is relatively high ($> 2\% \text{ cm}^{-1}$) over a 100 nm bandwidth centered at 480 nm, significant improvement in performance should be forthcoming as a result of pumping geometries which are better suited to optimization of the laser cavity.

Acknowledgements

This work was supported in part by the Office of Naval Research, The National Science Foundation and the Robert A. Welch Foundation.

References

1. Tittel, F. K., G. Marowsky, W. L. Nighan, Y. Zhu, R. A. Sauerbrey, and W. L. Wilson, Jr., "Injection Controlled Tuning of an Electron-Beam Excited XeF(C+A) Laser", IEEE J. Quantum Electron. (to be published, November 1986)
2. Nighan, W. L., R. A. Sauerbrey, Y. Zhu, F. K. Tittel, and W. L. Wilson, Jr., "Kinetically Tailored Properties of Electron-Excited XeF(C+A) and XeF(B+X) Laser Media Using an Ar-Kr Buffer Mixture", IEEE J. Quantum Electron. (to be published).
3. Marowsky, G., N. Nishida, H. Stiegler, F. K. Tittel, W. L. Wilson, Jr., Y. Zhu and W. L. Nighan, "Efficient Narrow Spectral Output in the Blue-Green Region from an Injection Controlled Electron Beam Excited XeF(C+A) Laser", Appl. Phys. Lett., Vol. 47, pp. 657-660, 1985.
4. Nighan, W. L., F. K. Tittel, W. L. Wilson, Jr., N. Nishida, Y. Zhu and R. A. Sauerbrey, "Synthesis of Rare Gas-Halide Mixtures Resulting in Efficient XeF(C+A) Laser Oscillation", Appl. Phys. Lett., Vol. 45, pp. 947-949, 1984.
5. Nachshon, Y., F. K. Tittel, W. L. Wilson, Jr., and W. L. Nighan, "Efficient XeF(C+A) Laser Oscillation Using Electron-Beam Excitation", J. Appl. Phys., Vol. 56, pp. 36-48, 1984.
6. Hsia, J., J. A. Mangano, J. H. Jacob, and M. Rokni, "Improvement in XeF Laser Efficiency at Elevated Temperatures", Appl. Phys. Lett., Vol. 34, pp. 208-210, 1979.
7. Mandl, A. E. and H. A. Hyman, "XeF Laser Performance for F₂ and NF₃ Fuels", IEEE J. Quantum Electron., Vol. QE-22, pp. 347-359, 1986.

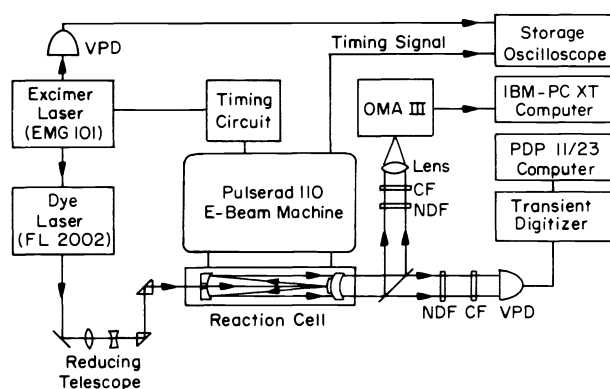


Figure 1. Schematic illustration of the experimental apparatus, showing in particular the unstable cavity optics inside the reaction cell, the tunable injection laser source, and the timing and data acquisition systems. OMA = Optical Multichannel Analyzer, VPD = Vacuum Photo Diode, CF = Color Glass Filter, NDF = Neutral Density Filter.

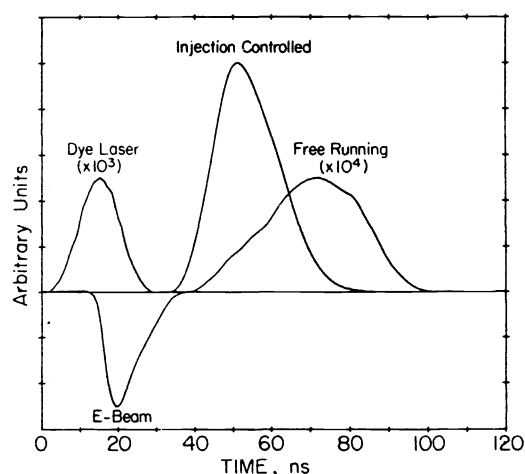


Figure 2. Temporal relationships of the dye laser, the e-beam excitation pulse, the amplified XeF(C+A) output, and the broadband XeF(C+A) output with the system operating as a free running oscillator.

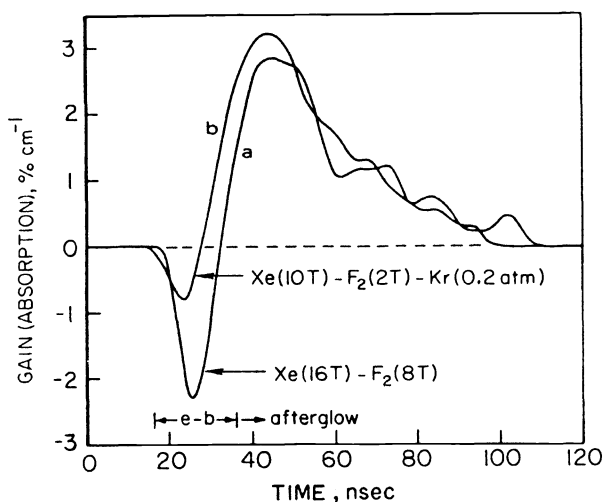


Figure 3. Temporal evolution of the XeF(C+A) net gain profile measured at 488 nm using an Ar-ion probe laser for mixture comprised of 6.5 atm Ar, 16 Torr Xe, 8 Torr NF₃ and 8 Torr F₂ (a), and 6.5 atm Ar, 10 Torr Xe, 8 Torr NF₃, 2 Torr F₂ and 150 Torr Kr (b).

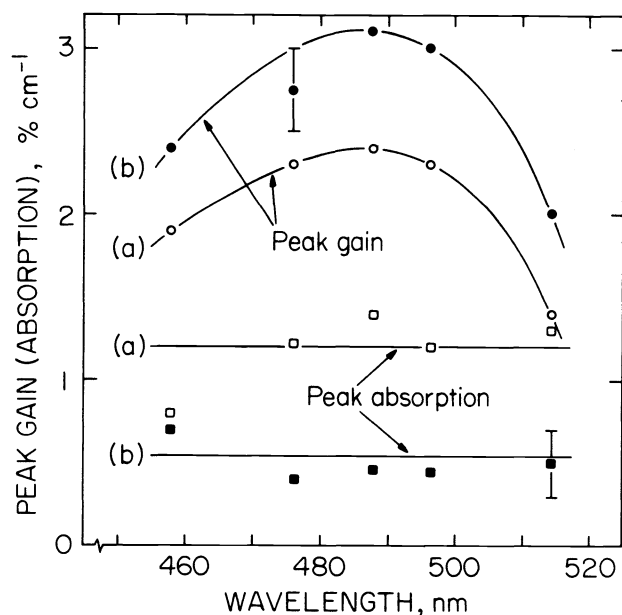


Figure 4. Wavelength dependence of the peak values of gain and initial absorption for mixtures comprised of 6.5 atm Ar, 16 Torr Xe, 8 Torr NF₃ and 8 Torr F₂ (a), and 6.5 atm Ar, 10 Torr Xe, 8 Torr NF₃, 2 Torr F₂ and 300 Torr Kr (b).

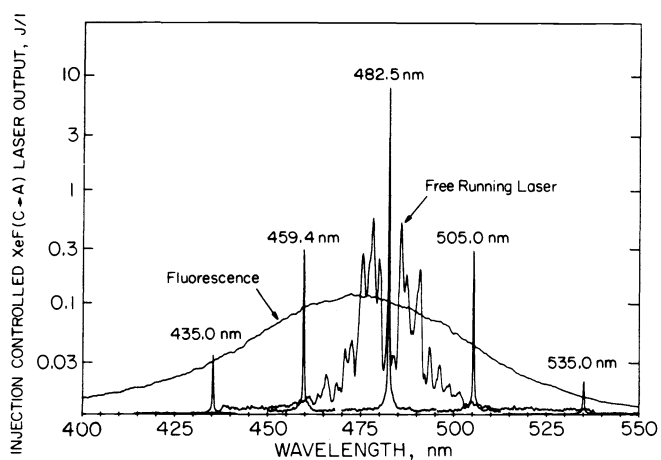


Figure 5. Qualitative comparison of superimposed time integrated spectra of the XeF(C+A) fluorescence, the injection controlled output of five separate shots at several wavelengths and a typical free running oscillator spectrum, all for representative conditions.

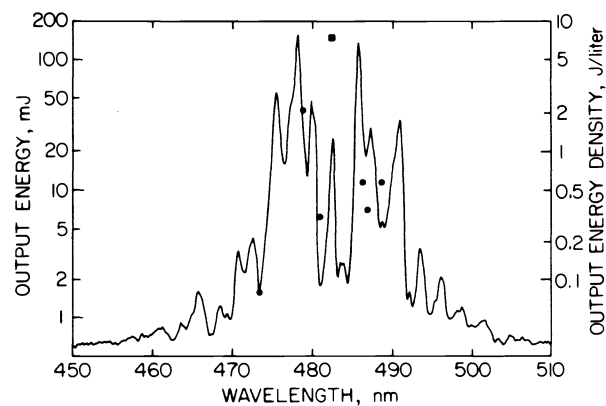


Figure 6. Measured amplified XeF(C+A) output energy for selected wavelengths for an injected dye laser pulse of approximately 1 mJ, along with a typical free running spectrum, the intensity of the latter in arbitrary units for comparison. The cavity M values were 1.05 (▲), 1.08 (■) and 1.14 (●).

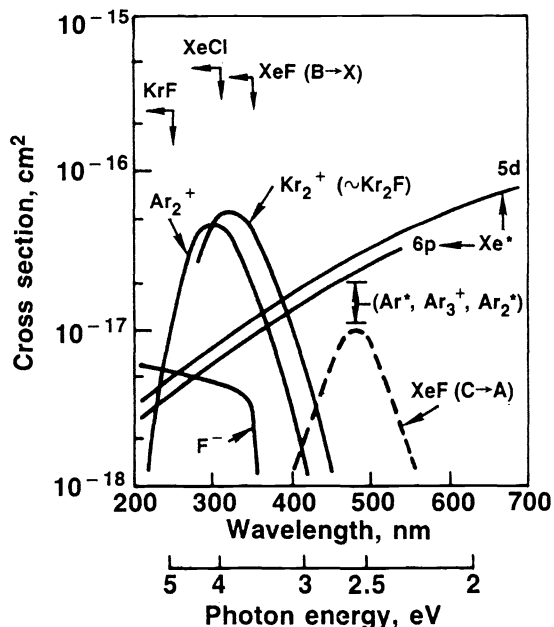


Figure 7. Cross sections for stimulated emission of the XeF(C+A) transition and the B+X transitions of XeF, KrF and XeCl. Also shown are the absorption cross sections of several transient species common to RGH laser mixtures.

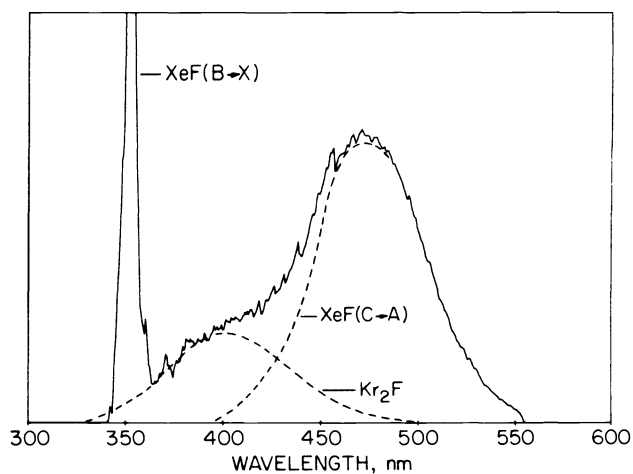


Figure 8. Time integrated fluorescence spectra for typical conditions indicating the individual contributions for Kr₂F and XeF and XeF(C+A).

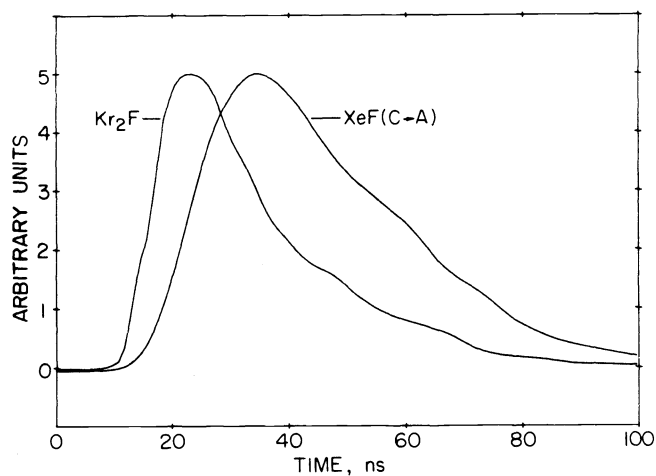


Figure 9. Normalized temporal evolution of the Kr_2F and $\text{XeF}(\text{C} \rightarrow \text{A})$ fluorescence spectra for the conditions of Figure 8.

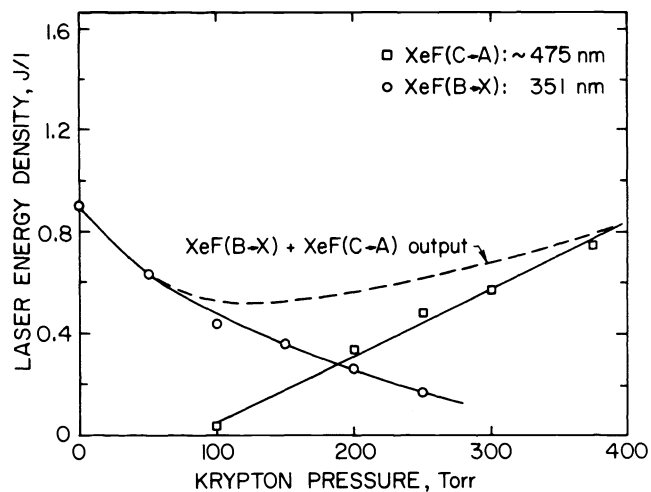


Figure 10. Measured laser pulse energy density for the simultaneously occurring $\text{B} \rightarrow \text{X}$ and $\text{C} \rightarrow \text{A}$ XeF excimer transitions in an e-beam excited mixture comprised of 6.5 atm Ar , 8 Torr Xe , 8 Torr NF_3 , 1 Torr F_2 and variable Kr pressure. The e-beam energy deposition was approximately 135 J/liter.